Electronic Supplementary Information for Surface structure and anion order of the oxynitride $LaTiO_2N$

Silviya Ninova and Ulrich Aschauer*

University of Bern, Department of Chemistry and Biochemistry, Bern, Switzerland.
**E-mail: ulrich.aschauer@dcb.unibe.ch; Tel: +41 031 631 5629*

Bulk

In addition to the models presented in the main text, other O/N orderings are also considered to exhaust all possible anion arrangements. In one of these (model 4*) we have *cis*-chains propagating one above the other in adjacent planes (see Figure S1). It has a slightly higher energy by 0.013 eV per formula unit (compare model 4 and model 4* in Table S1). The propagation of the chains in three dimensions (see model 3* in Figure S1) destabilises the structure by 0.035 eV per formula unit (compare model 3 and model 3* in Table S1). The energy differences between the lowest energy orderings are small, which can be reconciled with the absence of long range order in experiment.

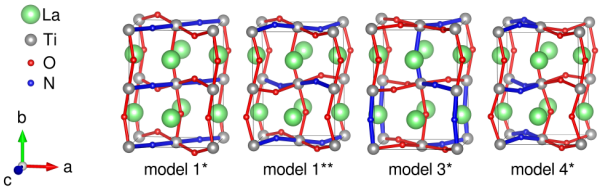

Figure S1 Additional O/N arrangement tested in the bulk unit cell

Table S1 Energy comparison (per formula unit) between the different models of $LaTiO_2N$ bulk as shown in Figure 1 of the main text and Figure S1. The band gaps are calculated at PBE+U level of theory. Values obtained using the hybrid functional HSE06 (x=0.18) are presented in parenthesis. The space group is determined after a relaxation of the geometry with a tolerance factor of 10^{-4} Å.

Models	Δ_{min} (eV)	Band gap (eV)		Space group
model 1	0.146	1.17	indirect	$P\bar{1}$
model 1*	0.146	1.17	indirect	$P\bar{1}$
model 1**	0.180	1.19	direct	$P\bar{1}$
model 2	0.311	1.16 (1.89)	direct	$P\bar{1}$
model 3	0.000	1.43	indirect	P1
model 3*	0.035	1.75	indirect	P1
model 4	0.000	1.43 (2.37)	indirect	P1
model 4*	0.013	1.22	indirect	$P\bar{1}$

Interestingly, the relaxation of the geometry along crystal axes with different octahedral rotation results in distinct structures, such as models 1 and 2 for instance. Model 1 almost completely straightens the small initial rotation along *c* from 6.3° to 0.7°. The same result is obtained in model 1*, where the Ti-N-Ti angle is along *a* (see Figure S1). Model 2, on the other hand, preserves the rotation along the most bent b axis, but this results in an even higher-energy structure. Interestingly, both structures retain the experimental symmetry, even though having only two rotational angles.

The 2D *cis*-anion arrangement of models 3 and 4, on the other hand, dictate that both O and N atoms are present along two crystal axes. Due to the different nature of the anions, this results in two different octahedral rotation angles (Ti-N-Ti and Ti-O-Ti) in those specific directions. The octahedral rotations, thus, cannot be determined unambiguously and directly compared to the experimental values.

Table S2 Bond lengths (Å) and octahedral rotations (°) of the most representative models for anion ordering in $LaTiO_2N$ bulk (see Figure 1 in the main text). The rotation angle is determined as (180-ϕ)/2, where ϕ is the angle Ti-X-Ti (X=N,O).

Models	Bonds		Octahedral rotation angle			Glazer notations[b]
	Ti-O	Ti-N	a	b	c	
model 1	2.014	2.019	0.7	14.8	14.8	$a^-b^+b^-$
model 2	2.000	2.026	9.9	9.9	12.3	$a^-a^+b^-$
model 3	1.983/2.017/2.063/2.117	1.936	8.7/12.6	14.0	8.7/12.6	$a^-b^+a^-$
model 4	1.983/2.063/2.117	1.936	8.7/12.6	8.7/12.6	14.1	$a^-a^+b^-$
experiment[a]	1.995/2.002,1.982-2.010		8.4	10.0	6.3	$a^-b^-c^-$

[a] S. J. Clarke, B. P. Guinot, C. W. Michie, M. J. C. Calmont and M. J. Rosseinsky, *Chemistry of Materials*, 2002, **14**, 288-294

[b] A. M. Glazer, *Acta Crystallographica Section B Structural Crystallography and Crystal Chemistry*, 1972, **28**, 3384-3392

In Table S3 we report the cell parameters for the different anion orderings (models 1-4) and compare them to the experimentally determined ones. In order to facilitate others to reproduce our results, in table S4, we also report the relaxed ionic coordinated for the different anion ordering models.

Table S3 Comparison between the cell parameters of the experimental bulk $LaTiO_2N$ structure and the relaxed models (see Figure 1 in the main text) describing different anion arrangements, lattice axes in (Å) and angles in °.

Models	a	b	c	α	β	γ
model 1	5.607	7.788	5.610	90.0	92.1	90.0
model 2	5.608	7.918	5.539	90.0	90.0	90.0
model 3	5.579	7.954	5.580	89.6	89.1	89.6
model 4	5.653	7.829	5.594	90.0	90.0	90.0
experiment[a]	5.610	7.872	5.575	90.2	90.2	90.0

[a] S. J. Clarke, B. P. Guinot, C. W. Michie, M. J. C. Calmont and M. J. Rosseinsky, *Chemistry of Materials*, 2002, **14**, 288-294

Table S4 Fractional coordinates of the atoms in the models of Figure 1 of the main text. The corresponding cell parameters are presented in S3

model 1

La	0.50073	0.24999	-0.00073
La	0.49927	0.75001	1.00073
La	1.00073	0.74999	0.49927
La	-0.00073	0.25001	0.50073
Ti	0.00000	0.00000	0.00000
Ti	0.50000	0.50000	0.50000
Ti	-0.00000	0.50000	-0.00000
Ti	0.50000	-0.00000	0.50000
O	0.93628	0.25000	1.06884
O	0.06372	0.75000	-0.06884
O	0.43628	0.75000	0.56884
O	0.56372	0.25000	0.43116
N	0.24993	-0.00314	0.25008
N	0.75007	1.00314	0.74992
N	0.74993	0.49686	0.75008
N	0.25007	0.50314	0.24992
O	0.24992	0.43374	0.74992
O	0.75008	0.56626	0.25008
O	0.74992	0.93374	0.24992
O	0.25008	0.06626	0.75008

model 2

La	0.49443	0.25000	-0.00001
La	0.50557	0.75000	1.00001
La	0.99443	0.75000	0.49999
La	0.00557	0.25000	0.50001
Ti	0.00000	0.00000	0.00000
Ti	0.50000	0.50000	0.50000
Ti	0.00000	0.50000	-0.00000
Ti	0.50000	0.00000	0.50000
N	0.92298	0.25000	0.99997
N	0.07702	0.75000	0.00003
N	0.42298	0.75000	0.49997
N	0.57702	0.25000	0.50003
O	0.25018	0.04322	0.24983
O	0.74982	0.95678	0.75017
O	0.75018	0.54322	0.74983
O	0.24982	0.45678	0.25017
O	0.25018	0.45681	0.75018
O	0.74982	0.54319	0.24982
O	0.75018	0.95681	0.25018
O	0.24982	0.04319	0.74982

model 3

La	0.49658	0.25527	0.01476
La	0.48562	0.74437	1.00383
La	0.99658	0.75527	0.51476
La	-0.01438	0.24437	0.50383
Ti	0.00427	0.00939	0.01498
Ti	0.50427	0.50938	0.51498
Ti	-0.01472	0.49037	-0.00403
Ti	0.48528	-0.00963	0.49597
N	0.95749	0.25005	1.04266
O	0.05374	0.75013	-0.05375
N	0.45749	0.75005	0.54266
O	0.55374	0.25013	0.44625
N	0.20723	-0.00005	0.29270
O	0.80366	0.99997	0.69611
N	0.70723	0.49995	0.79270
O	0.30366	0.49997	0.19611
O	0.20901	0.45630	0.70229
O	0.79712	0.54419	0.29045
O	0.70901	0.95631	0.20229
O	0.29712	0.04419	0.79045

model 4

La	0.48900	0.24089	0.00000
La	0.51100	0.74088	1.00001
La	0.98900	0.74089	0.50000
La	0.01100	0.24088	0.50001
Ti	-0.01901	-0.00538	0.00003
Ti	0.48099	0.49462	0.50003
Ti	0.01901	0.49462	0.00003
Ti	0.51901	-0.00538	0.50003
O	0.91190	0.25337	0.99996
O	0.08810	0.75337	0.00002
O	0.41190	0.75337	0.49996
O	0.58810	0.25337	0.50002
O	0.25009	0.05383	0.24989
N	0.74990	0.95729	0.75009
O	0.75009	0.55383	0.74989
N	0.24990	0.45729	0.25009
N	0.25010	0.45732	0.75009
O	0.74990	0.55381	0.24988
N	0.75010	0.95732	0.25009
O	0.24990	0.05381	0.74989

Table S5 Crystal coordinates of the high-symmetry k-points of the Brillouin zone used for the generation of the band structure shown in Figure 2 of the main text [a].

Models 1,3,4			
Γ	0.00000000	0.00000000	0.00000000
R	0.50000000	0.50000000	0.50000000
Y	0.00000000	0.50000000	0.00000000
X	0.50000000	0.00000000	0.00000000
Z	0.00000000	0.00000000	0.50000000
M	0.00000000	0.50000000	0.50000000
L	0.50000000	0.50000000	0.00000000
N	0.50000000	0.00000000	0.50000000
Model 2			
Γ	0.00000000	0.00000000	0.00000000
R	0.00000000	-0.50000000	0.50000000
Y	0.50000000	0.00000000	0.00000000
X	0.00000000	-0.50000000	0.00000000
Z	-0.50000000	0.00000000	0.50000000
M	0.00000000	0.00000000	0.50000000
L	0.50000000	-0.50000000	0.00000000
N	-0.50000000	-0.50000000	0.50000000

[a] W. Setyawan, S. Curtarolo, *Computational Materials Science* , 2010, **49** , 299-312

Surfaces

In Figure S2 surface models are shown that were omitted from Figure 3 in the main text.

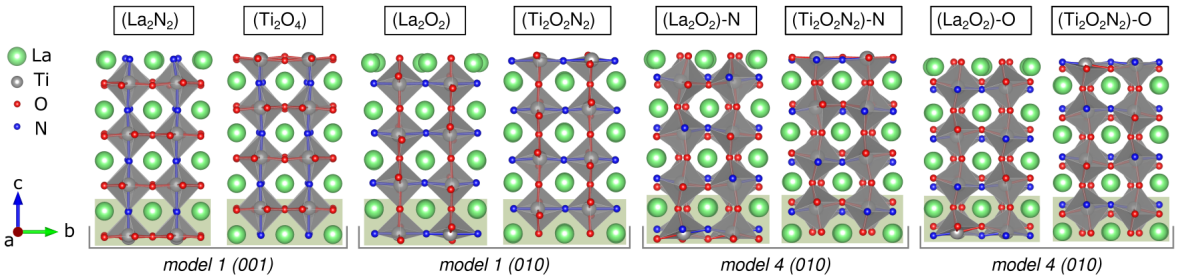

Figure S2 Optimised geometry of the surface slabs of models 1 and 4. The surfaces of the other models are presented in Figure 3 (main text). The bottom unit cell, highlighted in green, is kept fixed at bulk positions.

In the case of models with *trans* anion arrangement (models 1 and 2) as well as the *cis*-model 3, the surface slabs can be discriminated only by the chemical composition of the layers. For model 4, however, more subtle differences can be found. Within the Ti atomic layer, the N and O atoms are separated into sub-layers below or above the plane formed by the Ti ions. Such a geometry determines the proximity of the respective atoms to the surface and results in strong differences in surface energies (see Table 4 main text). In order to stabilise the already polar surfaces, different rumplings are observed as a result of the non-equivalent geometries, especially for the Ti termination (see Table S6). Indeed, while the N and O atoms still remain separated into sub-layers above and below the Ti-plane in $(Ti_2O_2N_2)$-O, they are at almost the same level in the corresponding $(Ti_2O_2N_2)$-N surface slab. This leveling-out of the anions is accompanied by a reduction in the interlayer distances.

Table S6 Geometry characteristics of the surface layers in all slab models (see Figures 3 in the main text and S2).

Model	Termination	Δ_{1-2} (%)[a]	Δ_{2-3} (%)[a]	s_O (Å)[b]	s_N (Å)[b]
model 1	(La_2O_2)	-8.6	6.3	0.358	-
	$(Ti_2O_2N_2)$	-8.2	7.1	0.352/-0.350	-0.081
	(La_2N_2)	-3.6	2.4	-	0.076/0.135
	(Ti_2O_4)	-8.6	3.6	0.080[c]	-
model 2	(La_2O_2)	-7.9	5.3	0.337	-
	$(Ti_2O_2N_2)$	-9.7	7.9	0.180/-0.399	0.071/-0.101
	(La_2N_2)	-2.5	4.1	-	0.104
	(Ti_2O_4)	-9.0	6.2	-0.053/0.204	-
model 3	(La_2NO)	-3.2	3.9	0.288	0.170
	(Ti_2O_3N)	-9.6	5.1	0.332/-0.220	0.076
model 4	(La_2O_2)-N	-4.6	2.8	0.258	-
	$(Ti_2O_2N_2)$-N	-9.5	7.5	0.061	-0.115
	(La_2O_2)-O	-7.1	4.7	0.387	-
	$(Ti_2O_2N_2)$-O	-7.0	5.6	-0.338	0.208

[a] The interplanar distances, Δ, are calculated as the difference between the averaged topmost atomic layer heights with respect to the bulk value.
[b] The rumpling, s, is calculated as the difference along z between the O or N atoms and the plane formed by the metal ones.
[c] The positions of the O atoms along z is variable.

Figure S3 shows a schematic view of the island, diagonal and trench reconstruction models we consider for our work.

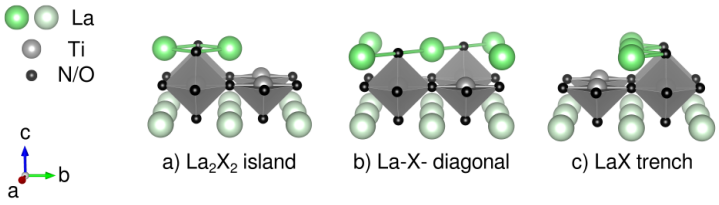

Figure S3 Schematic representation of the reconstruction models, based on the work of Deacon-Smith et al. *Adv.Mater.* 2014 ,**26** ,7252-7256, presented on a perfect cubic perovskite.

In Figure S4 we show additional reconstructed models that are less stable than the ones shown in Figure 5 in the main text. The corresponding surface energies are reported in Table 4 in the main text.

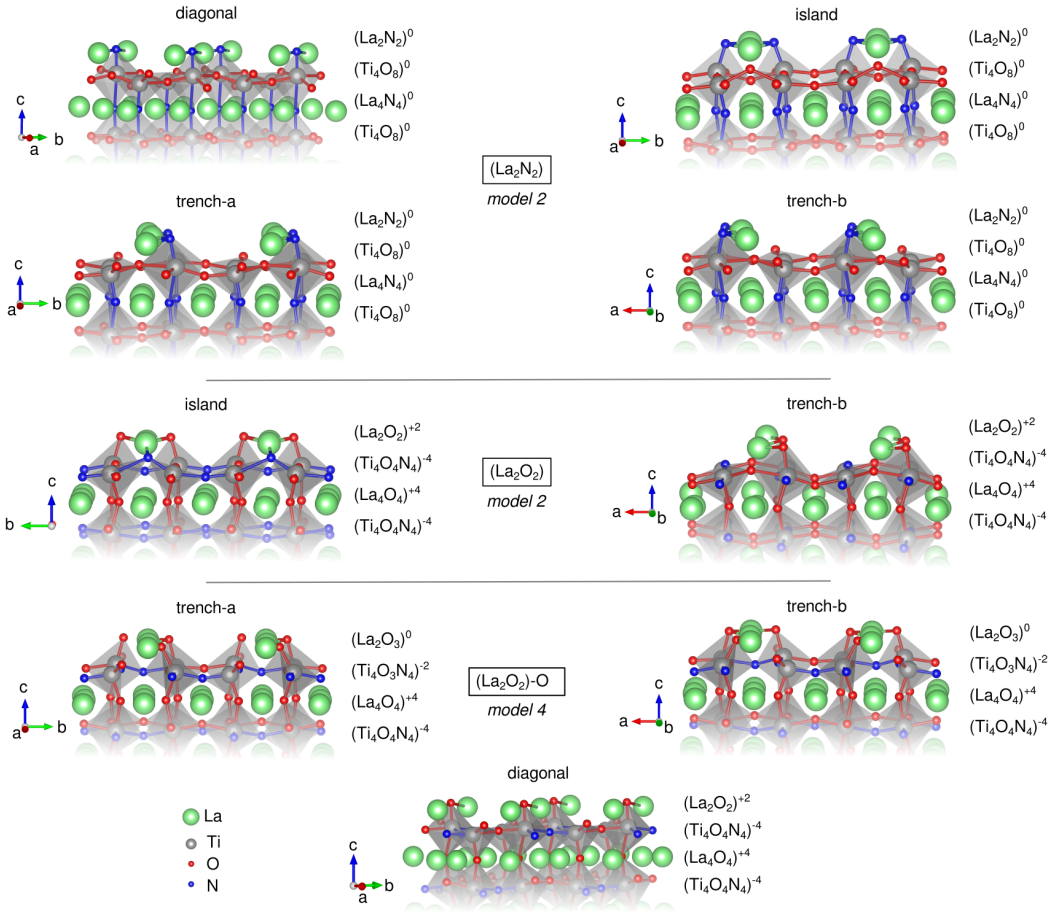

Figure S4 Geometry of some relaxed reconstructed models. The chemical composition for each layer is presented together with its formal charge. Those with the lowest surface energy can be found in Figure 5 (main text).